

## UC Davis

### UC Davis Previously Published Works

**Title**

Reversed DNA Strand Cleavage Specificity in Initiation of Cre-LoxP Recombination Induced by the His289Ala Active-site Substitution

**Permalink**

<https://escholarship.org/uc/item/7kb110b0>

**Journal**

Journal of Molecular Biology, 354(2)

**ISSN**

0022-2836

**Authors**

Gelato, Kathy A  
Martin, Shelley S  
Baldwin, Enoch P

**Publication Date**

2005-11-01

**DOI**

10.1016/j.jmb.2005.08.077

Peer reviewed

# Reversed DNA Strand Cleavage Specificity in Initiation of Cre–LoxP Recombination Induced by the His289Ala Active-site Substitution

Kathy A. Gelato<sup>1</sup>, Shelley S. Martin<sup>1</sup> and Enoch P. Baldwin<sup>1,2\*</sup>

<sup>1</sup>Section of Molecular and Cellular Biology, University of California Davis, 1 Shields Avenue, Davis, CA 95616 USA

<sup>2</sup>Department of Chemistry, University of California Davis, 1 Shields Avenue, Davis, CA 95616, USA

During the first steps of site-specific recombination, Cre protein cleaves and religates a specific homologous pair of LoxP strands to form a Holliday junction (HJ) intermediate. The HJ is resolved into recombination products through exchange of the second homologous strand pair. CreH289A, containing a His to Ala substitution in the conserved R-H-R catalytic motif, has a 150-fold reduced recombination rate and accumulates HJs. However, to produce these HJs, CreH289A exchanges the opposite set of strands compared to wild-type Cre (CreWT). To investigate how CreH289A and CreWT impose strand exchange order, we characterized their reactivities and strand cleavage preferences toward LoxP duplex and HJ substrates containing 8 bp spacer substitutions. Remarkably, CreH289A had different and often opposite strand exchange preferences compared to CreWT with nearly all substrates. CreH289N was much less perturbed, implying that overall recombination rate and strand exchange depend more on His289 hydrogen bonding capability than on its acid/base properties. LoxP substitutions immediately 5' (S1 nucleotide) or 3' (S1' nucleotide) of the scissile phosphate had large effects on substrate utilization and strand exchange order. S1' substitutions, designed to alter base-unstacking events concomitant with Cre-induced LoxP bending, caused HJ accumulation and dramatically inverted the cleavage preferences. That pre-formed HJs were resolved *via* either strand *in vitro* suggests that inhibition of the "conformational switch" isomerization required to trigger the second strand exchange accounts for the observed HJ accumulation. Rather than reflecting CreWT behavior, CreH289A accumulates HJs of opposite polarity through a combination of its unique cleavage specificity and an HJ isomerization defect. The overall implication is that cleavage specificity is mediated by sequence-dependent DNA deformations that influence the scissile phosphate positioning and reactivity. A role of His289 may be to selectively stabilize the "activated" phosphate conformation in order to promote cleavage.

© 2005 Elsevier Ltd. All rights reserved.

**Keywords:** tyrosine site-specific recombinase; Cre–LoxP recombination; strand exchange order; Holliday junction resolution; DNA cleavage specificity

\*Corresponding author

Abbreviations used: bp, base-pair(s); nt, nucleotide(s); CreWT, wild-type phage P1 Cre protein with N-terminal histidine tag inserted between Met1 and Ser2 (M<sub>1</sub>HHHHHHS<sub>2</sub>N<sub>3</sub>...); CreH289A, His<sub>6</sub>-Cre protein with the His289 to Ala substitution; CreH289N, His<sub>6</sub>-Cre protein with the His289 to Asn substitution; LoxP, 34 bp phage P1 recombination target site of Cre; sLoxP, 34 bp synthetic LoxP duplex; fLoxP, 220 bp restriction fragment containing LoxP (see Materials and Methods); 13 bp repeat, 13 bp inverted repeat sequence of LoxP that binds Cre protein; 8 bp spacer, 8 bp intervening sequence between the 13 bp repeats within which cleavage and rejoining occurs; 6 bp core, central 6 bp of LoxP that form heteroduplex after Cre-mediated recombination; S1 base, nucleotide 5' to the scissile phosphate in LoxP (the 14th nucleotide from either 5' end); S1' base, nucleotide 3' to the scissile phosphate in LoxP (the 15th nucleotide from either 5' end); S2' base, second nucleotide 3' to the scissile phosphate in LoxP (the 16th nucleotide from either 5' end); HJ, Holliday junction; HJ<sup>L</sup>, Holliday junction intermediate in Cre reactions arising from left arm-top strand exchange; HJ<sup>R</sup>, Holliday junction intermediate in Cre reactions arising from right arm-bottom strand exchange; PAGE, polyacrylamide gel electrophoresis.

E-mail address of the corresponding author: [epbaldwin@ucdavis.edu](mailto:epbaldwin@ucdavis.edu)

## Introduction

Bacteriophage P1 Cre protein is a member of the tyrosine recombinase/topoisomerase 1B family of DNA strand exchange proteins.<sup>1–4</sup> Tyrosine recombinases are characterized by a common chemical mechanism and a shared active-site structure that includes a tyrosine nucleophile and an Arg-His-Arg “catalytic triad” (Figure 1(a) and (b)).<sup>3,5–8</sup> Recombination requires only Cre and substrate DNA target site, LoxP (Figure 1(c)).<sup>9–11</sup> The simplicity and flexibility of the Cre–LoxP recombination system has made it particularly useful both for genome manipulation with nucleotide precision<sup>12–15</sup> and as a model system for studying tyrosine recombinase structure and function.<sup>16</sup>

Cre-mediated strand exchange at 34 bp LoxP sites involves two consecutive DNA cleavage and ligation steps and formation of a Holliday junction (HJ) intermediate (Figure 1(a)).<sup>17</sup> LoxP contains two inverted “13 bp repeat” Cre-binding sites flanking an “8 bp spacer”, the site of cleavage and religation (Figure 1(c)).<sup>9,18</sup> Two LoxP duplexes and four Cre protomers assemble into the active synaptic complex. Cleavage is effected by nucleophilic attack of active-site Tyr324 on a specific phosphodiester bond and its covalent attachment to the DNA 3′-phosphate. The cleaved 5′-end traverses the central void in the synaptic complex and displaces the tyrosine of the opposite covalent complex, forming the hybrid ligation product.

Cleavage is limited to one set of DNA strands by differentiation of the recombinase protomers into “cleaving” (competent for strand cleavage) and “non-cleaving” conformations. The first cleavage and ligation cycle, or “Initiation”, forms HJ intermediates with two homologous crossing-over strands bridging the Lox duplexes (Figure 1(a)). The second strand exchange, “Resolution”, occurs after the complex undergoes a “conformational switch” which interconverts the non-cleaving and cleaving subunit conformations. Resolution is essentially the inverse of initiation, and transforms the HJ into the duplex products. Each step is, in theory, reversible and the reaction is under equilibrium control.<sup>17,19–21</sup>

Recognition of LoxP asymmetry is required for correct alignment of the recombining DNA. The existing data and significance of this problem to site-specific recombination was recently reviewed by Lee & Sadowski.<sup>22</sup> This asymmetric recognition raises several questions: (i) are the top and bottom strands exchanged in a particular order; (ii) is this order required or only preferred to promote the complete reaction; and (iii) what are the protein–DNA interactions that enforce this order?

Accumulated evidence indicates that Cre does exchange LoxP strands in a specified order. Wild-type Cre/LoxP reactions (CreWT/LoxP) preferentially accumulate HJs arising from bottom strand (right-arm) cleavage,<sup>17,23–25</sup> implying that this strand was cleaved first. However, more top strand (left-arm) covalent intermediates accumulate with CreWT/LoxP,<sup>26</sup> top strand reactivity is greater for

suicide substrates,<sup>25,27</sup> and published CreWT/LoxP precleavage and HJ complex crystal structures show positioning of the cleaving subunit on the left arm, poised to cleave the top strand.<sup>27–29</sup> In a key experiment, we used a Cre mutant, with the His289Ala active-site substitution (CreH289A), as a model to determine strand cleavage preferences in CreWT/LoxP recombination, because it accumulated nearly all of its reacted substrate as HJ.<sup>27</sup> The HJ intermediates from CreH289A/LoxP reactions were formed almost exclusively through top strand cleavage. On the basis of these observations, we previously suggested that the left arm of LoxP was exchanged first.<sup>27</sup>

For CreWT, the DNA determinants of asymmetric strand cleavage for initiation and HJ resolution have also been investigated. Structural and biochemical data establish a key role for the nucleotide base 5′ to the cleavage site (the “S1 base”),<sup>25,30,31</sup> and for an asymmetric bend within the 8 bp spacer of LoxP when bound in the synaptic complex.<sup>21,26,28,31</sup> However, the exact relationships between S1 base recognition, bend position, and cleavage specificity are not clear. While base substitutions could alter DNA deformability and bend position within the spacer, previous work<sup>32,33</sup> indicated paradoxically that Cre is less sensitive to mutations in the central 6 bp of the LoxP spacer (the “6 bp core”).

In the work described below, we further investigated CreWT and His289 mutant reactivity and strand exchange preferences with LoxP variants containing 8 bp spacer substitutions. His289 was proposed to be the general acid/base for the tyrosine nucleophile/leaving group during recombination, and to coordinate the scissile phosphate thereby stabilizing the reaction transition states.<sup>16,19,28</sup> We demonstrated that the H289A mutation enabled Cre to preferentially cleave on the opposite arm of LoxP compared to CreWT, supporting that the active-site histidine functions in multiple roles during the recombination mechanism. Additionally, the 6 bp core, particularly the nucleotide 3′ to the scissile phosphate (the “S1′ base”), had a significant influence on cleavage preferences and reactivity. However, this influence was different between CreWT and CreH289A.

DNA deformations have been proposed to activate a particular scissile phosphate for cleavage.<sup>21,25,28</sup> Our working hypothesis is that activation requires precise scissile phosphate positioning for optimal interaction with active-site residues. The requisite positioning has a complicated dependence on the 8 bp spacer DNA sequence and the intermediate DNA state (duplex or HJ) that favor particular DNA deformations. His289 exerts cleavage specificity by selectively interacting with and stabilizing the “activated” scissile phosphate position by hydrogen bonding. In CreWT, the geometric constraints in the LoxP duplex promote right-arm cleavage, while in less-constrained HJ and suicide substrates, the cleavage specificity defaults to the left arm. In the absence of

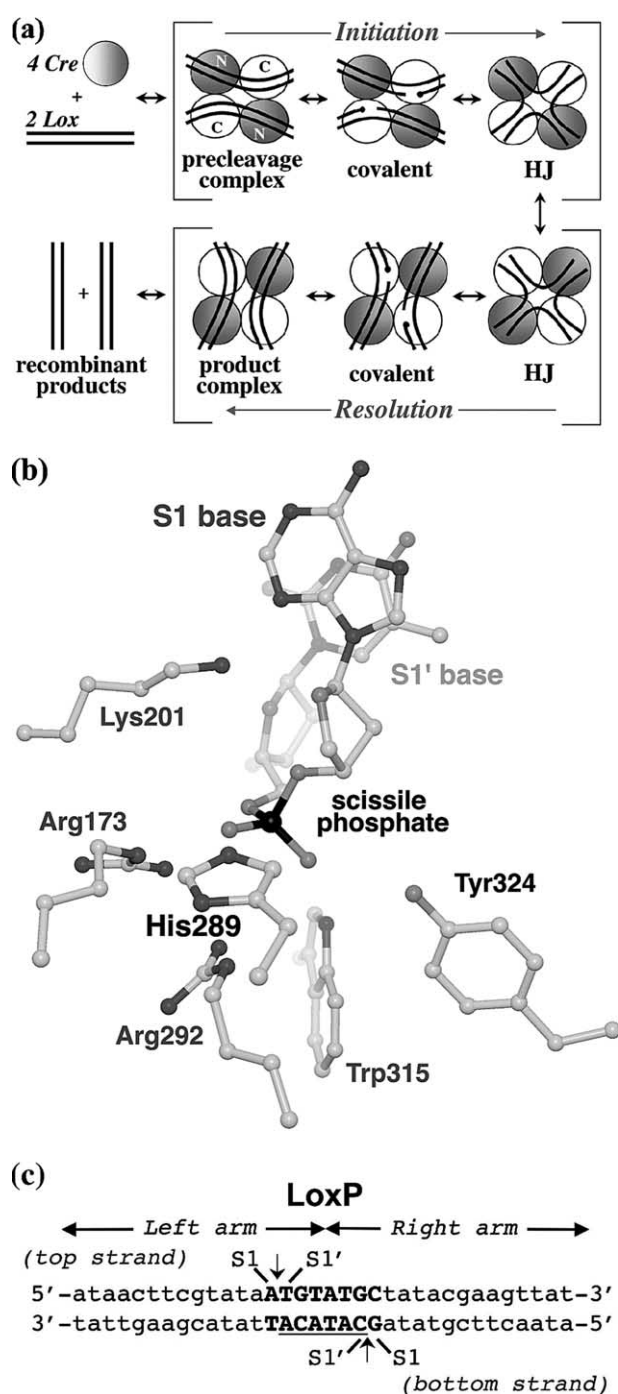


**Figure 1.** Recombination mechanism, His289 position, and LoxP substrate. (a) Cre/LoxP site-specific recombination mechanism. Two Cre monomers bind one LoxP site (parallel black lines). Two Cre<sub>2</sub>LoxP dimers associate to form the synaptic complex, with each Cre monomer having one of two conformations: the cleaving subunits (white, C) are positioned to initiate recombination and covalent attachment to the LoxP scissile phosphate (black circles), while the non-cleaving subunits (gray, N) become activated for cleavage prior to the HJ resolution step (see Introduction). Brackets separate the “initiation” and “resolution” reactions. An asymmetric bend is depicted within LoxP adjacent to the cleavage site; multiple lines of evidence support a bend upon Cre binding, but its position is controversial. (b) His289 position within the cleaving Cre subunit active site, in

His289, the altered energy landscape favors the default specificity.

## Results

### Cre His289 mutants have reduced catalytic activity and accumulate HJ intermediates

Our earlier results with CreH289A/LoxP motivated us to further characterize the effects of His289 substitutions. We compared the catalytic and complex assembly competence of CreWT, CreH289A and CreH289N by quantitatively following HJ intermediate and product formation as a function of complex concentration or time.<sup>34</sup> In these experiments, intermolecular recombination of an end-labeled 220 bp Lox-containing restriction fragment (*fLoxP*) with a synthetic 34 bp LoxP substrate (*sLoxP*) yields 141 bp and 113 bp labeled duplex products and an intermediate “chi” structure, corresponding to the HJ complex (Figure 2(a) and (b)).

As observed earlier,<sup>27</sup> CreH289A/LoxP significantly reduced the amount of substrate reacted (turnover efficiency) compared to CreWT/LoxP, and, while CreWT generated mostly products, CreH289A predominantly accumulated HJs (Figure 3(b) and Table 1). Consistent with disrupting catalysis, the His289Ala substitution also reduced the overall LoxP turnover rate 150-fold. While CreWT/LoxP exhibits two exponential phases that differ sevenfold in rate,<sup>34</sup> CreH289A/LoxP exhibited a single phase with 45-fold smaller rate constant than the CreWT/LoxP slow phase. CreH289A also had reduced affinity for LoxP, with the apparent  $K_D$  of active complex formation 2.8-fold higher than CreWT/LoxP (Table 2). Although the His289 side-chain is just beyond hydrogen-bonding distance in precleavage and HJ structures,<sup>20,21,27,28</sup> it apparently contributes to protein–DNA interactions that lead to substrate turnover.

a HJ complex.<sup>27</sup> Substitutions at this site (CreH289A and CreH289N) result in reduced recombination rates and increased HJ accumulation. The S1 and S1' bases flank the scissile (cleavage) phosphate, which is proximal to conserved tyrosine recombinase active-site residues: nucleophile Tyr324, and Arg173, Lys201, Arg292, and Trp315. (c) 34 bp recombination substrate. LoxP is nearly symmetric owing to its pair of 13 bp inverted repeat Cre-binding sequences (lower case), but possesses an asymmetric 8 bp intervening sequence within which DNA cleavage and rejoining occur (8 bp spacer, bold upper case). The central 6 bp core is the segment of DNA that is physically exchanged (underlined). The S1 base is immediately 5' to the scissile phosphate, and the S1' and S2' bases are 3' to the scissile phosphate. The overall asymmetry results in different strands being exchanged depending on which arm is bound by the cleaving Cre subunits.

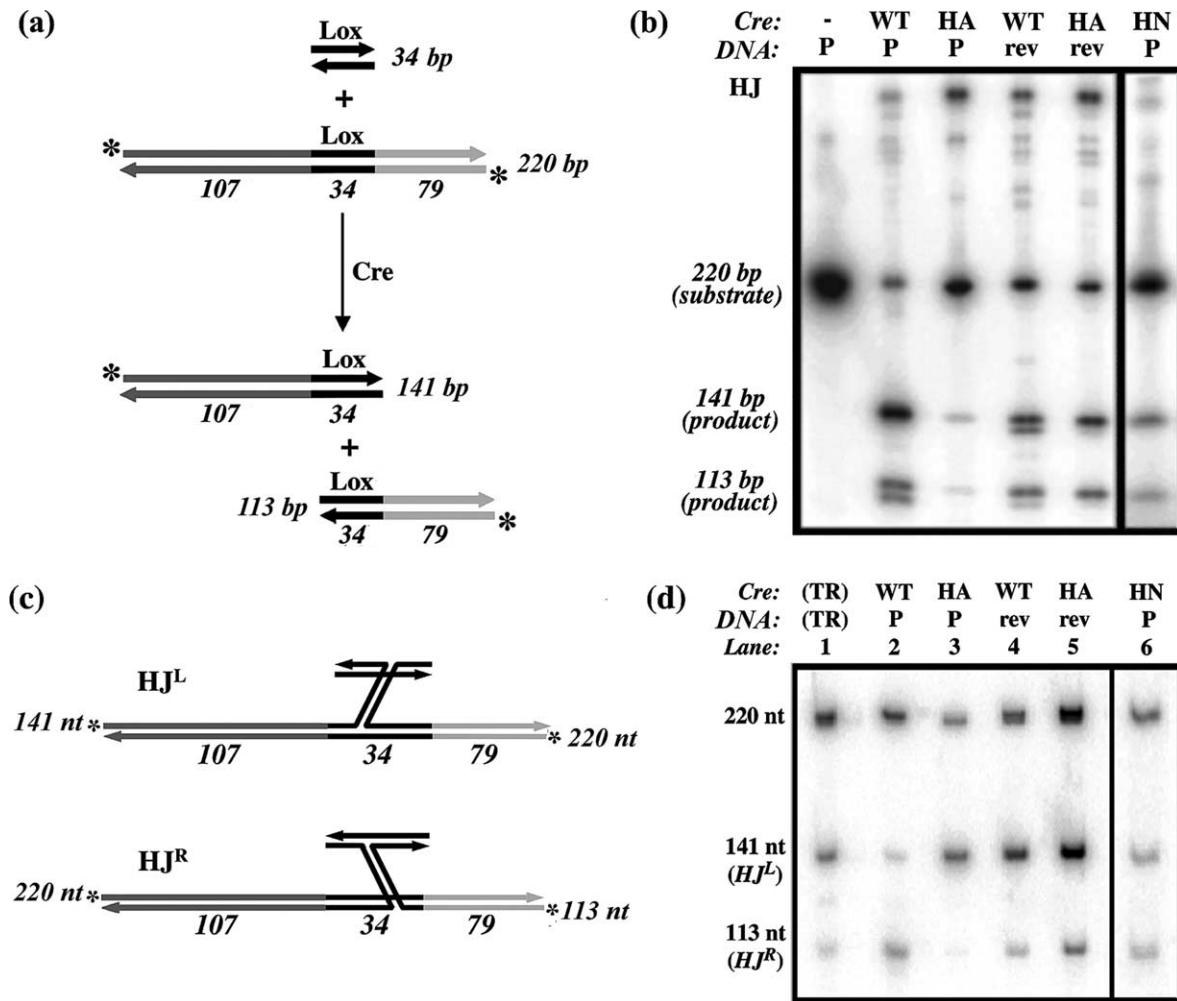


**Figure 2.** *In vitro* recombination assays. (a) Intermolecular Cre/Lox recombination. 34 bp unlabeled Lox duplex (sLox) is mixed with  $^{32}\text{P}$  5' end-labeled (\*) 220 bp Lox-containing duplex (fLox). Reaction with Cre yields 141 bp and 113 bp labeled products, and HJ complexes. The length of each DNA arm to the Lox site is indicated. (b) Analysis of reaction products by SDS-PAGE and phosphorimaging. The enzymes used in these representative reactions were CreWT (WT), CreH289A (HA), and CreH289N (HN). Lox substrates were either LoxP (P) or S1rev (rev, see Figure 3(a)). Unreacted Lox substrate is 220 bp; products are 141 bp and 113 bp. HJ intermediates (HJ) are seen as a slower migrating band. Doublet 141 and 113 bands were detected only in CreWT reactions, and are products of Proteinase K digestion of covalent intermediates. (c) HJ polarity determination. The HJ labeled-strand composition depends on the strand exchanged during initiation. HJs arising from initial left-arm (top strand) exchange will have labeled strands (\*) of 220 and 141 nt ( $\text{HJ}^{\text{L}}$  diagram). HJs resulting from initial right-arm (bottom strand) exchange will have labeled strands of 220 nt and 113 nt ( $\text{HJ}^{\text{R}}$  diagram). (d) Analysis of accumulated HJ intermediates. Labeled strands of HJs purified from reactions in (a) were visualized by denaturing PAGE. Lane 1 contains an aliquot from a CreWT/LoxP total reaction (TR), for use as size markers.

The more conservative His289Asn substitution had modest effects. Significantly, CreH289N/LoxP produced recombination products but, compared to CreWT/LoxP, had lower turnover efficiency and accumulated more of the reacted material as HJ (Figure 3(b) and Table 1). The reaction was skewed toward the slow phase, and the overall rate was 15 times slower than CreWT, but CreH289N had a similar affinity for LoxP compared to CreWT (Table 2). These results indicate that although His289 is a significant contributor to reaction kinetics, its acid-base function is not crucial for recombination, but its hydrogen-bonding potential may be a more important factor. The persistence and minor

perturbation of the fast phase in CreH289N/LoxP reactions suggests that hydrogen bonding is particularly important to this subreaction (Table 2).

We do not know why less substrate is utilized by His289 mutants. Reduced turnover efficiencies are observed in reactions with poorer-binding Lox substrates<sup>34</sup> (K.A.G., unpublished data). "Misaligned" complexes, those in which the 8 bp spacer regions are aligned in the incorrect parallel orientation, may also contribute to the lower yields but are not detected by the methods used here. Indeed, the high-energy mismatched HJ and products arising from such complexes were not observed (see Experimental validation of HJ analysis for details).

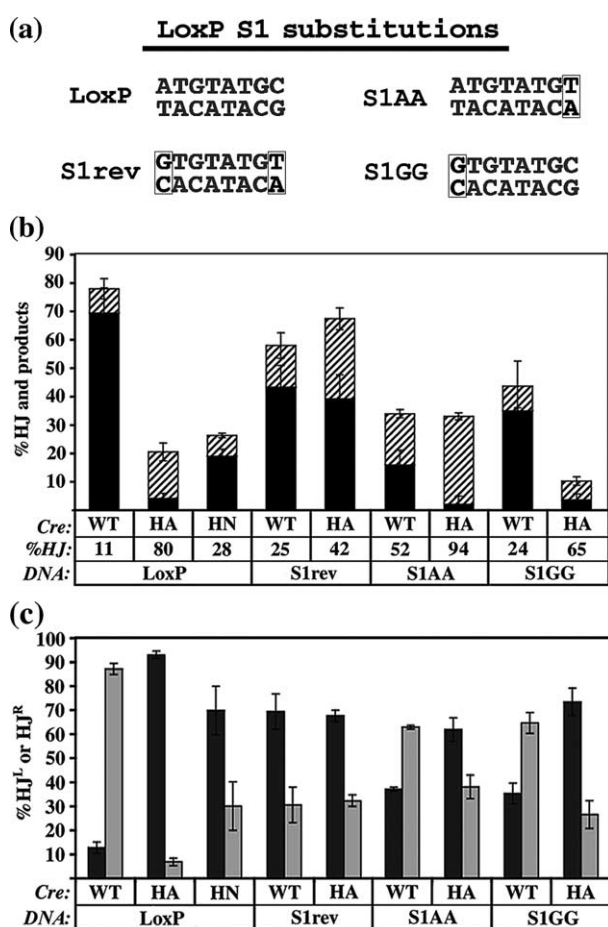


**Figure 3.** Substrate turnover and Holliday junction polarities with Lox substrates. (a) 8 bp spacer sequences of LoxP S1 mutants. The S1 bases are swapped in S1rev, while the S1 bases are symmetrized in S1AA and S1GG substrates. The spacer substitutions are highlighted (black outline). (b) Quantitation of substrate turnover. SDS-PAGE band intensities were measured using autoradiography. Each bar indicates the total substrate turnover, which is the sum of product formation (black segment) and HJ intermediate accumulation (hatched segment), as percentages of total counts in substrate, HJ, and products bands. Error bars denote the standard deviation of 3–7 reactions. Enzymes and substrates are indicated, and the relative percentage of HJ as a fraction of the total substrate reacted ( $\%HJ = 100 \times HJ / (HJ + \text{products})$ ) is calculated. (c) Quantitation of HJ polarity. Band intensities for HJ<sup>L</sup> (dark gray bars) and HJ<sup>R</sup> (light gray bars) were quantified using denaturing PAGE and phosphorimaging. Values are expressed as a percent of total counts of the 141 nt and 113 nt bands, and are corrected for the unequal labeling of the fLox 5' DNA ends (see Materials and Methods). Error bars denote the standard deviation of three reactions.

### CreH289A has altered strand cleavage preferences with differently constrained LoxP substrates

We determined the polarity of HJ intermediates accumulated in intermolecular recombination

reactions, to infer which strand is preferentially exchanged during initiation. In reactions with unlabeled *sLox* and <sup>32</sup>P-labeled *fLox* substrates, this preference is determined from the size of the labeled HJ DNA. HJs resulting from LoxP left-arm exchange (HJ<sup>L</sup>) have labeled strands of 141 and 220 bp, and HJs resulting from right-arm exchange (HJ<sup>R</sup>) have 113 and 220 bp labeled DNA strands (Figure 2(c) and (d)). Although this method is a standard measure of initiation strand exchange preference,<sup>17,23–25,27,35</sup> an important caveat is that accumulated HJ polarities are not a direct measure of actual strand initiation preferences, and it is not possible to determine the contribution of each initiation event to product formation. Indeed, it could be argued that HJ<sup>L</sup> or HJ<sup>R</sup> accumulate because they are poorer substrates for resolution rather than being preferred for initiation. However, if Cre utilizes differential strand specificities for initiation and resolution to drive the reaction “forward”,<sup>25</sup> then CreWT preference for left-arm HJ resolution is consistent with preferred right-arm initiation.

With CreWT/LoxP, the HJ polarity, expressed as the HJ<sup>L</sup>:HJ<sup>R</sup> ratio, is maintained over the course of the reaction and is independent of temperature (see Experimental validation of HJ analysis for details). Further, after 16 h, CreWT<sub>4</sub>LoxP<sub>2</sub> complexes retain all of the properties of those that are freshly prepared. Thus, the HJs are not isolated from off-pathway dead-end complexes, and the rate-limiting reaction steps occur before HJ formation.

The Cre His289 mutants accumulated LoxP HJ complexes with opposite polarity compared to CreWT (Figures 2(d) and 3(c), and Table 1). CreWT HJs arose predominantly from right-arm strand exchange (1:6.8 HJ<sup>L</sup>:HJ<sup>R</sup>, this work) but CreH289A HJs resulted from almost exclusive left-arm exchange (13.4:1 HJ<sup>L</sup>:HJ<sup>R</sup>), a 90-fold reversal between CreWT and CreH289A. Similar to CreH289A, CreH289N also accumulated HJ<sup>L</sup>, but only a 16-fold reversal in preference compared to CreWT. This result contrasts those for other Cre mutants which accumulated HJs, but predominantly of the HJ<sup>R</sup> form.<sup>17,35</sup>

Not only do CreWT and CreH289A reactions accumulate different proportions of HJ<sup>L</sup> and HJ<sup>R</sup>, they resolve HJs with different strand preferences. To measure HJ resolution cleavage biases, we reacted pre-formed HJs with CreWT and CreH289A and quantified the duplex products arising from left arm-top strand and right arm-bottom strand exchange.<sup>30</sup> An 87 bp labeled product indicates resolution *via* the left arm, and a 75 bp labeled product indicates HJ resolution on the right arm (Figure 4(a)). Consistent with previous work,<sup>17,30</sup> CreWT resolved LoxP HJs at a ratio of 3.5:1 left:right-arm exchange. CreH289A turned over approximately one-third as much LoxP HJ and exhibited a greater left arm bias compared to CreWT, with a 7:1 preference for left-arm resolution (Figure 4(b)). In other words, CreH289A was less reactive toward LoxP HJ and preferentially

**Table 1.** LoxP and mutant substrate reactivity and HJ polarities with Cre

Substrate	% Reaction extent <sup>a</sup>		Absolute %HJ accumulation <sup>b</sup>		HJ <sup>L</sup> :HJ <sup>R</sup>	
	CreWT	CreH289A	CreWT	CreH289A	CreWT	CreH289A
LoxP <sup>c</sup>	78±6	20±3	8.6±3.4	16±1	1:(6.8±0.7)	(13±1):1
S1rev	58±2	67±6	15±4	28±4	(2.3±0.7):1	(2.1±0.2):1
S1AA	34±4	33±2	18±5	31±3	1:(1.7±0.1)	(1.6±0.4):1
S1GG	44±9	10±3	8.6±1.1	6.7±2.1	1:(1.8±0.3)	(2.8±0.5):1
S1 <sub>L</sub> ' - G	70±2	58±1	42±2	54±1	1:(11±1)	1:(4.9±0.2)
S2 <sub>L</sub> ' - T	30±8	2±1	3.2±0.6	1.0±0.5	1:(9.2±2.2)	(3.9±1.4):1
S1 <sub>R</sub> ' - A	42±1	59±3	13±3	58±3	(7.3±2.0):1	(106±23):1
S2 <sub>R</sub> ' - C	57±4	9±2	9.3±1.8	8.5±1.9	1:(2.8±0.1)	(20±3):1

<sup>a</sup> Percentage substrate turned over, i.e. converted from substrate to HJ or products.

<sup>b</sup> Absolute percentage HJ accumulation is the HJ band intensity as a fraction of substrate-derived counts per lane.

<sup>c</sup> Results for CreH289N/LoxP: % reaction extent, 26±2; absolute %HJ accumulation, 7.4±0.8; HJ<sup>L</sup>:HJ<sup>R</sup> (2.3±1.5):1.

**Table 2.** Cre complex assembly and reaction turnover parameters with LoxP, S1rev, and LoxP<sub>sui</sub>

Enzyme	Substrate	Binding parameters <sup>a</sup>			Kinetics parameters <sup>b</sup>		
		<i>f</i> , extent	<i>K<sub>D</sub></i> (nM)	$\alpha$ , Hill	<i>A</i>	<i>k<sub>1</sub></i> (10 <sup>3</sup> s <sup>-1</sup> )	<i>k<sub>2</sub></i> (10 <sup>3</sup> s <sup>-1</sup> )
CreWT <sup>c</sup>	LoxP	67±8	58±13	2.1±0.8	0.42±0.02	4.5±1.3	32±3
CreH289A	LoxP	19±3	160±23	2.3±0.2	1	0.10±0.004	-
CreH289N	LoxP	24±1	53±8	2.9±0.2	0.68±0.04	0.43±0.2	24±1
CreWT	S1rev	58±2	58±11	1.8±0.4	0.41±0.02	2.2±0.2	61±4
CreH289A	S1rev	68±7	102±3	2.8±0.4	0.75±0.01	0.15±0.01	2.7±0.2
CreH289N	S1rev	36±4	42±4	2.7±0.3	0.43±0.04	0.31±0.05	14±1
<i>Suicide substrate (LoxP<sub>sui</sub>)<sup>b</sup></i>							
CreWT <sup>c</sup>	L*+R	28±5	-	-	0.78±0.07	3.0±1.0	120
CreWT <sup>c</sup>	R*+L	7±1	-	-	0.61±0.10	3.3±0.6	120
CreH289A	L*+R	40±5	-	-	1	0.43±0.06	-
CreH289A	R*+L	3.4±0.5	-	-	1	0.30±0.04	-

<sup>a</sup> *K<sub>D</sub>* and Hill coefficients were determined using the modified Hill equation:  $v' = f \{ ([\text{complex}]/K_D)^{\alpha} / [1 + ([\text{complex}]/K_D)^{\alpha}] \}$ , as previously described.<sup>34</sup> [*v'*, observed percentage of substrate reacted; *f*, maximum percent of substrate that can react (reaction extent); *K<sub>D</sub>*, apparent dissociation constant;  $\alpha$ , apparent Hill coefficient].

<sup>b</sup> *A*, *k<sub>1</sub>* and *k<sub>2</sub>* were calculated by fitting kinetics data to the bi-exponential function:  $v'(t) = f \{ 1 - [A e^{-k_1 t} + (1-A)e^{-k_2 t}] \}$ , as previously described.<sup>34</sup> [*t*, time from reaction start until quenching; *v'*, 100 – the percent of substrate unreacted; *f*, percent of substrate reacted at an infinite time (reaction extent); *A* and *k<sub>1</sub>*, amplitude and rate constant for the slow phase; *k<sub>2</sub>*, rate constant for the fast phase].<sup>34</sup> A single-phase reaction is indicated by amplitude (*A*) = 1.

<sup>c</sup> Data from Martin *et al.*<sup>27,34</sup>

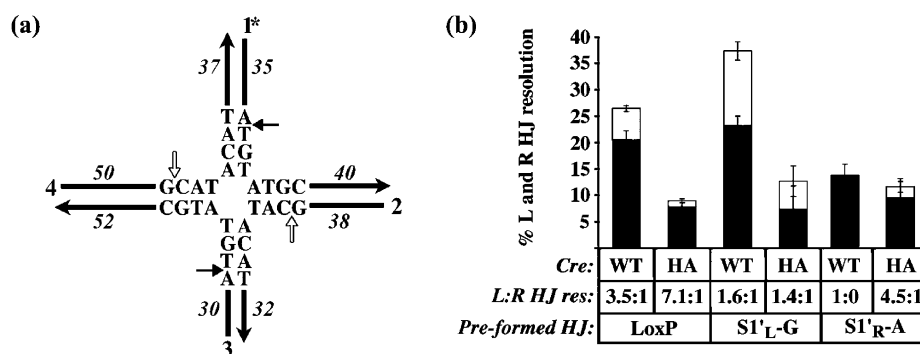


**Figure 4.** Pre-formed HJ resolution strand preferences. (a) Pre-formed synthetic HJs. Lox-containing oligonucleotides 1–4 were annealed to make pre-formed HJs.<sup>30</sup> Strand lengths are: 1 = 75 nt, 2 = 70 nt, 3 = 82 nt, 4 = 87 nt; the length of each arm to the cleavage site is indicated adjacent to each strand. Strand 1 (1\*) was 5' end-labeled, so that cleavages on the left arms (black arrows) yield an 87 bp labeled duplex product, while cleavages on the right arms (white arrows) yield a 75 bp labeled duplex product. (b) HJ resolution preferences. The percent of left-arm (black bar) and right-arm (white bar) HJ cleavage products were quantified using PAGE and phosphorimaging. The total height of each bar indicates the percentage of pre-formed HJ resolved. Error bars denote the standard deviation of three reactions. The enzyme, pre-formed HJ substrate, and ratio of left:right-arm HJ resolution (L:R HJ res) are listed. S1<sub>L</sub>' - G and S1<sub>R</sub>' - A substrates have S1' spacer bases substituted as shown in Figure 6(b).

resolved it toward the “reactants”, providing a partial explanation for why CreH289A/LoxP accumulates HJ intermediates.

The different cleavage biases exhibited by CreWT with LoxP duplex and HJ substrates suggest that the LoxP bridging DNA strands induce unique constraints in the initiation and resolution complexes. To measure strand cleavage preferences in the absence of these influences, we utilized the half-site suicide substrate LoxPsui.<sup>27</sup> This substrate traps covalent Cre–Lox complex intermediates after a single cleavage event by virtue of specific DNA nicks one base-pair 3' to the cleavage site on each strand<sup>36</sup> (Figure 5(a)). As visualized by SDS-PAGE, slow-migrating covalent Cre–DNA complexes are formed if cleavage occurs on the left arm with L\* + R substrates or on the right arm with R\* + L substrates (Figure 5). The ratio of covalent complexes formed in each reaction can be taken as a measure of “intrinsic cleavage bias” for each DNA strand, because the nicks presumably also remove bridging strand constraints on scissile bond positioning. With LoxPsui, CreH289A exhibited a 12-fold bias for left-arm cleavage over right-arm cleavage, greater than the fourfold left arm preference exhibited by CreWT<sup>27</sup> (Figure 5(b)). Similar to CreWT, CreH289A formed left and right arm covalent complexes with LoxPsui at approximately equal rates, but 100-fold more slowly and were described by only a single reaction phase (Table 2). Without constraints imposed by continuous DNA in duplex substrates, both CreWT and CreH289A favor left-arm cleavage. However, the left and right arms are cleaved at the same rate. As in CreWT/LoxP initiation, in which HJ<sup>R</sup> and HJ<sup>L</sup> also formed at the same rate, strand selection does not occur at the rate-limiting step.

### The role of the S1 base in LoxP strand selection

Crystal structures reveal that Lys86 and Lys201 make the only direct contacts with the LoxP spacer

bases, specifically at the S1 positions.<sup>16,27,28</sup> S1 base identities contribute to initiation and HJ resolution strand exchange bias, and their influence is seen dramatically using S1rev, a Lox substrate in which the left and right arm S1 bases are swapped (Figure 3(a)).<sup>25,30</sup> Because CreH289A has an altered LoxP recognition mechanism compared to CreWT, we tested whether S1rev would influence cleavage preferences of CreH289A.

Reversing the S1 base identities had differential and opposite effects on CreWT and CreH289A reactivity (Figure 3(b), and Tables 1 and 2), the most noteworthy being that CreH289A/S1rev yielded significant recombination products with a smaller proportion of accumulated HJ. CreH289A turned over more S1rev than LoxP, with a twofold greater rate. In contrast, CreWT/S1rev turned over less substrate than CreWT/LoxP, but also with a doubled rate. A lower proportion of reacted substrate was converted to recombination products, and instead accumulated as HJ. CreH289A had higher affinity for S1rev than for LoxP, whereas CreWT maintained the same affinity for both substrates.

S1 base reversal affected HJ polarity differently with CreWT and CreH289A (Figure 3(c) and Table 1). CreWT accumulated HJ<sup>L</sup> with S1rev, as observed earlier,<sup>25</sup> while CreH289A similarly accumulated HJ<sup>L</sup>. In other words, CreWT preferred to form junctions from cleavage at S1-Gua on the right arm of LoxP and the left arm of S1rev, while CreH289A accumulated HJs from left-arm initiation with both substrates. Nonetheless, these differences still represent significant polarity change for both proteins, a 15.6-fold reversal for CreWT and a 6.4-fold reduced bias for CreH289A.

### Contribution of the LoxP 6 bp core to strand selection

While results with S1rev indicate a strong S1 base role, we wanted to determine the importance of

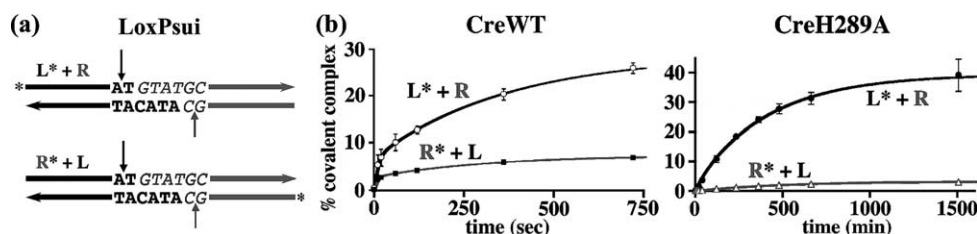


**Figure 5.** CreWT and CreH289A covalent complex formation, using a LoxP suicide substrate. (a) Suicide substrate. LoxPsui<sup>27</sup> contains a nick in the DNA backbone between the S1' and S2' bases, adjacent to the cleavage sites (vertical arrows), to trap covalent Cre–Lox complexes.<sup>36</sup> The left arm (L) duplex DNA (black lines, spacer sequence in bold) was annealed with the right arm (R) duplex DNA (gray lines, spacer sequence in italics), with <sup>32</sup>P-labeling on either the left arm (L\*) or the right arm (R\*). Left arm covalent complex formation is measured in L\* + R reactions; right-arm covalent complex formation is measured in R\* + L reactions. (b) CreWT and CreH289A reactivity with LoxPsui. Covalent complex formation time-course of L\* + R (black curves) and R\* + L (gray curves) suicide substrate reactions, with CreWT (left panel, seconds time scale)<sup>27</sup> or CreH289A (right panel, minutes time scale). Total covalent complex formed as a function of time was determined as described in Materials and Methods, and the data fit to the function detailed in Table 2, which lists the relevant kinetic parameters for each fit. Error bars indicate the standard deviation of three reactions.



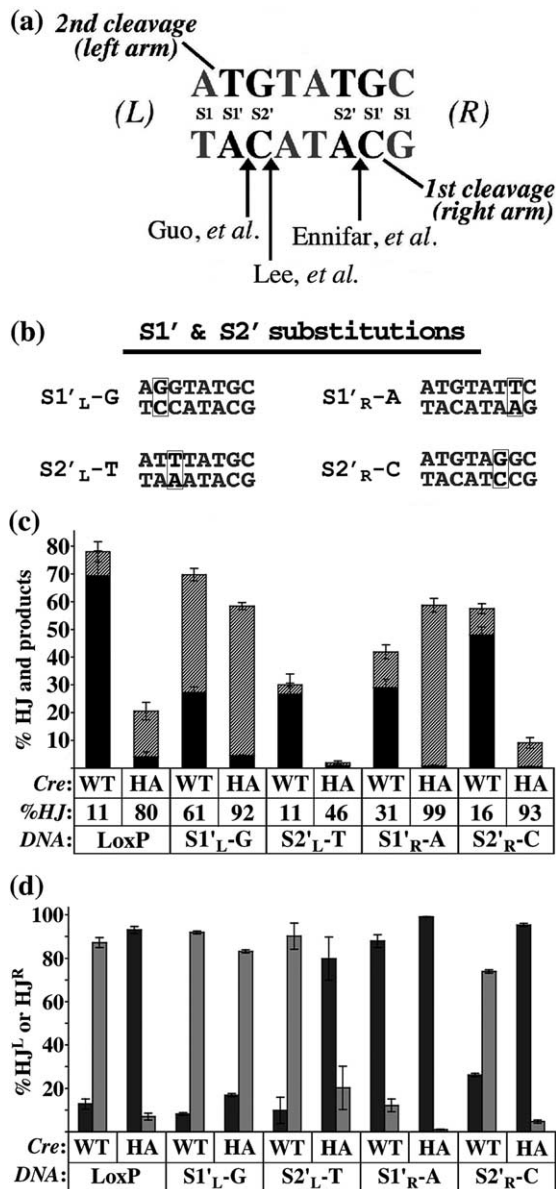


**Figure 6.** Reactivity and HJ polarity with Lox S1' and S2' mutant substrates. (a) Proposed base-steps involved in CreWT-induced bending of LoxP based on structures of precleavage complexes<sup>21,28</sup> or substrate circular-permutation mobility shift experiments.<sup>31</sup> Within the precleavage complex, LoxP is predicted to have a kink at various base steps within the 8 bp spacer (arrows), according to the model that CreWT cleaves the LoxP right arm first (cleavage sites are indicated). We made substitutions at the S1' and S2' sites (black) on the left (L) and right (R) arms, to potentially alter base stacking interactions and DNA deformability of the S1/S1'/S2' base steps. (b) 8 bp spacer sequences of LoxP S1' and S2' mutants. The S1' and S2' substitutions (black outline) are 3' to a scissile phosphate, within the 6 bp core. (c) Lox substrate turnover by CreWT and CreH289A, quantified by SDS-PAGE and phosphorimaging. Total substrate turnover (bars), product formation (black segment) and HJ intermediate accumulation (hatched segment) are reported as absolute percentages of total counts in substrate, HJ, and products bands. Error bars denote the standard deviation of three reactions. Enzymes, substrates, and the percentage of HJ as a fraction of the total

the remainder of the 8 bp spacer, the 6 bp core. To accomplish this, we symmetrized the S1 bases, leading to S1AA and S1GG substrates<sup>30</sup> (Figure 3(a)), and determined the reactivities and HJ strand compositions in CreWT and CreH289A-mediated reactions.

With CreWT, both substrates were less efficiently utilized and accumulated a greater fraction of HJ compared to LoxP, but S1GG was more reactive than S1AA (Figure 3(b) and Table 1). In contrast, CreH289A reacted greater amounts of S1AA, but 94% of this material still accumulated as HJs. S1GG was a poorer substrate than LoxP, accumulating less HJ but a similar amount of recombinant products. Thus, substrate utilization preferences were inverted, so that CreWT had a greater reaction extent with S1GG than S1AA, while S1AA was the more reactive substrate with CreH289A.

With CreWT, symmetrizing the S1 bases reduced the right-arm HJ polarization by approximately fourfold, compared to LoxP (Figure 3(c) and Table 1). With CreH289A the left-arm HJ<sup>L</sup> bias was also reduced, but polarization was less with S1AA than with S1GG. Interestingly, these ratios are comparable to that for CreH289A/S1rev, suggesting a large non-additive S1 base contribution for CreH289A. These results support that the 6 bp core alone exerts a moderate strand bias in initiating recombination, but its influence on CreH289A is again clearly opposite that of CreWT.

### The role of the S1' and S2' bases in strand selection

Since Cre contacts only the phosphate backbone of the 6 bp core,<sup>21,27,28</sup> recognition of 8 bp spacer sequence asymmetry occurs partially through "indirect readout". Synaptic complex structures,<sup>21,28</sup> cleavage specificity for bulged Lox substrates,<sup>26</sup> and circular permutation/phasing analyses<sup>31</sup> point to a role for a DNA distortion, particularly an asymmetric bend, within the 8 bp spacer (Figure 6(a)).

We attempted to alter LoxP spacer deformation energetics at the most flexible TpG/CpA S1'/S2' base steps, by converting them to more rigid TpT/ApA or GpG/CpC base steps (Figure 6(b)).<sup>37,38</sup> The S1' substitutions influence both the S1/S1' and the S1'/S2' base steps, while the S2' substitutions influence the S1'/S2' and the S2'/S3' base steps. The substitutions also change local base-pair stabilities, which may influence other DNA

substrate reacted (%HJ) are listed. (d) Quantitation of HJ polarity. As described in Figure 3(c), accumulated HJs were analyzed by denaturing PAGE. Band intensities for HJ<sup>L</sup> (dark gray bars) and HJ<sup>R</sup> (light gray bars) were quantified using phosphorimaging. Values are expressed as a percentage of total counts of the 141 and 113 nt bands, and are corrected for the slightly unequal labeling of the fLox 5' DNA ends. Error bars indicate the standard deviation of three reactions.

deformations. For example, the G16/C19 base-pair separation observed in a Cre-LoxP HJ complex<sup>27</sup> would be favored by the S2'<sub>L</sub> – T substitution, due to the weaker T16/A19 base-pair. These spacer substitutions dramatically altered reaction extents, product distributions and HJ polarities (Figure 6(c) and (d), and Table 1), but elicited different responses from CreWT and CreH289A. Three patterns emerge from comparisons of CreWT and CreH289A.

First, HJ polarization reversals occurred when the substituted bases were proximal to the scissile bond preferred for LoxP initiation by each protein. CreWT/S1'<sub>R</sub> – A substrate turnover was reduced twofold with somewhat more HJ accumulation. The HJ<sup>L</sup> majority product represented a 50-fold polarity reversal from the HJ<sup>R</sup> accumulated with CreWT/LoxP. In reactions with CreH289A, S1'<sub>L</sub> – G was much more reactive but still accumulated 92% of the reacted substrate as HJ<sup>L</sup>. Strikingly, HJ<sup>R</sup> accumulated instead of HJ<sup>L</sup>, a 50-fold inversion of CreH289A/LoxP preference. However, unlike S1rev, S1'<sub>L</sub> – G was unable to induce CreH289A to generate significant product, even though the initiating cleavage occurred on the right arm.

Second, reactions with substrates that were S1'-substituted on the arm preferred for LoxP HJ resolution<sup>30</sup> (see Figure 4(b)) accumulated a greater proportion of HJ with enhanced polarity bias. CreWT/S1'<sub>L</sub> – G reacted to a similar extent as CreWT/LoxP, but accumulated fivefold more HJ with twice the bias for HJ<sup>R</sup>. Similarly, CreH289A was three times more reactive towards S1'<sub>R</sub> – A than LoxP, and accumulated essentially all of the reacted substrate as HJ<sup>L</sup>.

Third, CreH289A was much more sensitive than CreWT to S2' substitutions. CreWT/S2'<sub>R</sub> – C was minimally perturbed, with normal product levels but a greater proportion of HJ<sup>L</sup> than CreWT/LoxP. CreWT/S2'<sub>L</sub> – T turned over less substrate, but the polarity of accumulated HJs was essentially that of CreWT/LoxP. Like CreWT, CreH289A utilized S2'<sub>R</sub> – C similarly to LoxP, but unlike CreWT, it did not turn over S2'<sub>L</sub> – T.

We also characterized the CreWT and CreH289A HJ resolution biases using S1'-substituted substrates (Figure 4(b)). For CreWT, which favored left-arm LoxP-HJ resolution,<sup>30</sup> resolution of S1'<sub>R</sub> – A yielded left arm exchange product. These data suggest that reduced product formation in CreWT/S1'<sub>R</sub> – A is likely due to increased "misinitiation" *via* left-arm cleavage, and the resulting HJ<sup>L</sup> accumulation is due to the inability to resolve *via* right-arm cleavage, similar to CreH289A/LoxP. In this view, the products that were observed with CreWT/S1'<sub>R</sub> – A occurred *via* "normal" right-arm initiation. With CreH289A, which resolved LoxP HJ *via* the left arm twice as readily as CreWT, the S1'<sub>R</sub> – A substitution had little effect. On the left arm, S1'<sub>L</sub> – G increased overall HJ reactivity with both enzymes, but reduced strand bias. The increased reactivity indicates the reduced bias was not due to inhibited

left-arm cleavage, but rather enhanced right-arm HJ resolution.

Overall, these reactivity patterns suggest that CreH289A senses different conformational properties than CreWT in both initiation and HJ resolution. The discrepancy between cleavage biases in initiation and resolution, that is, when HJs are accumulated but the preformed HJs are resolved with reasonable efficiency, implies that the complexes are less able to switch strand specificities *via* isomerization.<sup>35</sup>

## Discussion

These results illustrate an enigmatic relationship between a Cre catalytic substitution and DNA cleavage specificity in Cre-Lox recombination. Substituting both His289 and LoxP bases near the cleavage site induced complex and inter-related changes in rates, outcomes, and strand cleavage order, suggesting that they act in concert during crucial reaction steps. CreWT initiates on the LoxP right arm, but the left arm is preferred for cleavage in "unconstrained" suicide and HJ substrates,<sup>25,27,30</sup> and covalent complex formation.<sup>26</sup> These results provide support for the idea that, for LoxP, there is an intrinsic bias for left-arm cleavage, but due to restrictions imposed by duplex substrate strand continuity, right-arm cleavage is favored in initiation.<sup>25</sup> The overall implications for Cre-LoxP recombination are that the CreWT reaction is driven "forward" by differential strand cleavage specificity for duplex and HJ DNA, and that this specificity is a complicated function of Lox sequence.<sup>22</sup>

His289Ala resulted in large rate reductions, less tight LoxP binding, and increased HJ accumulation. This behavior is in marked contrast to that of yeast Flp His305 "step-arrest" mutants which accumulate covalent intermediates in both initiation and resolution reactions,<sup>39,40</sup> suggesting that the general acid role (tyrosine displacement) of His305 is more critical than its general base role (tyrosine attack) in FLP-Frt recombination. His289 hydrogen bonding potential, rather than proton transfer capability, appears to be crucial for the overall recombination reaction since CreH289N exhibited a moderate turnover defect and normal binding affinity. His289 does not differentiate Lox DNA sequences by direct base interactions. Instead, its side-chain forms a hydrogen bond with the scissile phosphate oxygen in the covalent intermediate complexes,<sup>19,28</sup> but is 4–5 Å distant in precleavage and HJ complexes.<sup>20,21,27–29</sup> By implication, it likely coordinates the scissile phosphate prior to or during recombination initiation, and this coordination seems to be a reasonable axis by which the Lox 8 bp spacer sequence modulates recombination activity and cleavage specificity.

## Interplay of cleavage specificity and HJ accumulation

Unexpectedly, the His289Ala substitution markedly altered Cre strand cleavage preferences with all DNA substrates. CreH289A responses to 8 bp spacer substitutions generally imitated those of CreWT reactions, but with opposite polarity. For LoxP, CreH289A's enhanced left-arm preference prevails not only in the initiation but also in HJ resolution and suicide substrate cleavage. Thus while CreWT displayed differential strand specificity in initiation and resolution, CreH289A preferred the same strand in both, explaining its proclivity for HJ accumulation.

CreH289A/S1rev behavior provides support for this idea. With its greater tendency to initiate S1rev recombination *via* right-arm cleavage, CreH289A produced substantial product and accumulated much less HJ. We suggest that product could be produced by two different pathways. In one scheme, CreH289A produces HJ<sup>L</sup> *via* 6 bp core-driven initiation, evidenced by the fact that it prefers to initiate S1AA and S1GG on the left arm, and this HJ<sup>L</sup> is then resolved by isomerization and right-arm cleavage driven by the Lys86/Lys201 interactions with S1-Ade. Alternatively, CreH289A initiates *via* the right-arm S1-Ade, followed by left-arm HJ<sup>R</sup> resolution, possibly promoted by the 6 bp core. In either case, accumulation of S1rev HJs would reflect initiation on the alternative strand with the persistent inability to isomerize and resolve the resulting HJs to products. As His289 interacts similarly with DNA in the non-cleaving and cleaving subunits of the HJ complexes,<sup>20,27</sup> it is not structurally obvious why the His289Ala substitution would block HJ isomerization. As a particularly salient example, CreH289A efficiently initiated on the S1<sub>L</sub>'-G right arm and exhibited a bias toward resolving S1<sub>L</sub>'-G HJ *via* left-arm cleavage, but still accumulated HJs. Thus, "correct" initiation by CreH289A on the right arm is not sufficient to promote completion of the recombination reaction, further implying that this mutant is isomerization-defective.<sup>35</sup> The higher HJ accumulation levels could be further explained by CreH289A binding more tightly to HJs relative to duplex substrates, compared to CreWT.

## DNA determinants of cleavage preference

The S1 base and 6 bp core influence strand exchange bias for both proteins, albeit in different ways. Comparisons of LoxP, S1AA or S1GG, and S1rev substrates suggest an approximate fourfold influence of S1-Gua for directing CreWT initiation. S1AA and S1GG initiation biases indicate an approximate twofold further right-arm preference from the 6 bp core. Interestingly, even these preferences are inverted with CreH289A. S1-Ade contributes to CreH289A left-arm initiation in LoxP, but has little effect on right-arm initiation, and hence CreH289A exhibits similar left-arm cleavage preferences for S1rev, S1AA, and S1GG substrates.

This particular specificity for S1-Ade is implied by its apparent modulation of the 6 bp core contribution, since CreH289A/S1GG has a threefold left arm preference while CreH289A/S1AA has only a 1.5-fold preference.

The CreWT left-arm preference in HJ resolution has been attributed to Lys86<sup>25,30</sup> or Lys201<sup>27</sup> hydrogen bonds with the S1-Ade base observed in crystal structures, but there are no obvious structural correlates to its right-arm initiation preference. Crystallographic and biochemical evidence suggest that an asymmetric bend facilitated by unstacking specific base steps directs the initiating cleavage to a particular scissile phosphate.<sup>21,24,26,28,31</sup> S1'/S2' bases are unstacked in the precleavage complexes,<sup>21,28</sup> implicating this base-step as critical. Indeed, S1<sub>L</sub>'-G and S1<sub>R</sub>'-A substitutions had much stronger effects on cleavage bias and reactivity than those caused by the S1 substitutions, contrasting previously reported results.<sup>32</sup> However, the mild effects of S2' mutations on CreWT cleavage compared to S1 and S1' substitutions imply that the S1/S1' base step is more important.

With either CreWT or CreH289A, base unstacking perturbations had the greatest effect when they occurred on the same arm as the initiating or HJ-resolving cleavage event. Enhanced left-arm cleavage of CreWT/S1<sub>R</sub>'-A is consistent with blocking right-arm initiation while the buildup of HJ<sup>R</sup> in CreWT/S1<sub>L</sub>'-G is consistent with blocking left-arm cleavage during HJ resolution. Similarly, CreH289A/S1<sub>L</sub>'-G reversed initiation bias is consistent with perturbing an unstacking event involving either the S1/S1<sub>L</sub>' or S1/S2<sub>L</sub>' base steps. The latter base-step is more likely important, since the S2<sub>L</sub>'-T substitution inhibited HJ and product formation. Thus, CreH289A and CreWT strand preferences are directed both by different LoxP arms and by different spacer base steps, pointing to a fundamental divergence in how each protein recognizes the spacer region. The results leave little doubt that CreH289A is not a good model for studying CreWT initiation<sup>27</sup> but instead has a unique specificity that was unexpected for a catalytic mutant.

## Potential mechanisms of strand selection and a role for His289

When is the choice of cleavage strand made? The time-independence of the CreWT/LoxP HJ polarities suggest that cleavage preferences are not exerted in the rate-limiting step, although it is still possible that differential cleavage or religation rates drive strand preferences in steps that are invisible in the present assay procedures. For the same reason, the biphasic reaction kinetics are not related to initiation cleavage preferences in CreWT/LoxP.

How do DNA deformations influence strand cleavage preference and how is His289 involved? Two models for strand selection are equally supported by the data. In the "Conformational Control Model", cleaving Cre subunits associate randomly with either LoxP arm, but one of the scissile

phosphates can more easily attain the “activated” geometry that promotes cleavage. In the “Assembly Model” cleaving and non-cleaving Cre subunit conformations are imposed during complex assembly, determined by the S1 base interaction and/or 8 bp spacer deformation energetics. The cleaving subunit position in the initiation complex determines the strand that is cleaved.

We favor the Conformational Control Model because the scissile phosphate positions in existing precleavage and HJ complex structures<sup>20,21,27–29</sup> do not depict a cleavage-competent active site since the scissile phosphate is only partially engaged with the active-site residues.<sup>22,28</sup> We suggest that a prerequisite for cleavage is repositioning the phosphate to optimize interactions with the active site, in this case hydrogen bonds with His289, as well as Arg173, Arg292, and Trp315. A nearby DNA “kink” has been suggested to activate the scissile phosphate for cleavage,<sup>28</sup> but any number of DNA deformations could contribute to phosphate repositioning. The frequency of attaining the optimal position would be governed by DNA fluctuations that are biased by the 8 bp spacer disposition, which is influenced by sequence-dependent DNA deformation energetics, and by the electrostatic/hydrogen bonding environment provided by Cre. Due to their proximity, the energetic dependences of S1/S1' base stacking geometry would be expected to be a prime contributor, but these would be further modulated by the different 8 bp spacer strand positions in the precleavage and HJ complexes.

We propose that the energy landscape of unconstrained LoxP substrates favors fluctuations that promote left-arm cleavage. With CreWT, direct His289 side-chain/scissile phosphate contacts combined with restrictions imposed by duplex substrate strand continuity favor scissile phosphate trajectories for right-arm cleavage. Without His289, and/or with non-duplex substrates, the left-arm “intrinsic specificity” for LoxP is dominant.

Evidence for interplay between the 8 bp spacer DNA sequence, His289, and Cre cleavage preferences is provided by the CreWT/S1<sub>R</sub><sup>1</sup> – A reaction which partially imitated CreH289A/LoxP. HJ<sup>L</sup> accumulated to much higher levels, presumably because CreWT misinitiated on the left arm and was unable to isomerize. Recombination products that did arise may have formed from a fraction of substrate undergoing “normal” right-arm initiation followed by the highly preferred left-arm S1<sub>R</sub><sup>1</sup> – A HJ resolution.

For the Conformational Control Model, majority right-arm initiation would be achieved if complexes with left arm-associated cleaving subunits could reassemble into right arm-associated ones on a time scale that is not rate-limiting, as implied by our preincubation experiments (see Experimental validation of HJ analysis). It should also be noted that if the contributors to cleavage activation in the Conformational Control Model instead direct asymmetric loading of the cleaving subunit on LoxP, the data are also consistent with the Assembly Model. In either scenario, His289 has

both pre-catalytic and catalytic roles in Cre–Lox recombination.

## Materials and Methods

### Proteins, Lox substrates, and <sup>32</sup>P-labeling

Wild-type Cre (CreWT) and CreHis289Ala (CreH289A) were expressed and purified as described, each with an N-terminal His<sub>6</sub> tag.<sup>27,41</sup> CreHis289Asn (CreH289N) was generated by the Kunkel<sup>42</sup> method and was purified analogous to CreWT. Synthetic 34 bp oligonucleotides (sLox) were obtained from MWG Biotech, and the 220 bp Lox-containing DNA fragments (fLox) were prepared and 5'-end <sup>32</sup>P-labeled as described earlier.<sup>27</sup> Labeled fLox substrates were digested with BamHI to determine the relative labeling efficiency of the left and right DNA arms. Lox sequences are detailed in Figures 3(a) and 6(b).

### Lox substrate reactivity and HJ polarity

Reactions were performed as described, with 3–7 replicates.<sup>27</sup> Briefly, 4800 nM Cre was reacted with 1200 nM sLox and 10 nM labeled fLox, for 15–17 h at 21 °C in optimized reaction buffer.<sup>41</sup> Reactions were quenched in 1% (w/v) SDS, 0.5 mg/ml Proteinase K for 1–2 h at 37 °C, and products analyzed on SDS-10% polyacrylamide gels.<sup>43</sup> Gels were vacuum-dried (1 h, 80 °C), exposed to a Fuji BAS-MS 2040 image plate, and scanned with an image plate reader (Molecular Dynamics Storm 860). Bands were visualized and intensities quantified using Molecular Dynamics ImageQuant.

For HJ intermediate analysis, reaction samples were separated by 1.5 mm preparative SDS-PAGE. HJ bands were excised following exposure to film, and gel slices were crushed and soaked for 16 h at 21 °C in 450 μl of 100 mM ammonium acetate (pH 7), 0.5 mM EDTA, and 1 μg of carrier oligonucleotide. Extracts were passed through a 0.2 μm filter and precipitated with 900 μl ethanol. Dried DNA pellets were resuspended in 90% (v/v) formamide in TE buffer and 0.01% (w/v) bromophenol blue, heat-denatured at 95 °C, and the component strands separated by 10% PAGE with 8 M urea and Tris–borate–EDTA (TBE) buffer. Gels were dried and band intensities quantified after exposure to an image plate. HJ labeled strand compositions were adjusted to account for the relative <sup>32</sup>P-labeling efficiency of the left and right DNA arms, by analysis of BamHI restriction digest products of fLox.

In reactions where more than one slow-migrating labeled DNA species was detected, we determined that each represented HJ complexes, with nearly identical labeled strand composition. This result was seen most notably in CreWT/S1GG reactions, which had three distinct HJ bands with different mobilities, all of which contained HJ<sup>L</sup>:HJ<sup>R</sup> in the same ratio.

### Experimental validation of HJ analysis

In our assay, Cre/Lox HJ complexes that are unable to undergo a second round of strand exchange cannot be differentiated from complexes that are capable of completing the reaction. In experiments to test the assumption that HJ polarities accurately reflect fluxes through right-arm initiation and left-arm initiation pathways, we followed the HJ<sup>L</sup>:HJ<sup>R</sup> ratio over 15 s to 16 h, and over a range of 5–37 °C. We also determined the reactivity of complexes over 16 h by preincubating stoichiometric

sLoxP substrate with CreWT overnight before addition of labeled fLoxP and measuring reaction kinetics. HJ polarity did not change with time or temperature, and preincubation kinetics were essentially the same as in the standard reaction in which there was no preincubation time (data not shown). Given the large excess of unlabeled sLoxP (1200 nM), labeled fLoxP (10 nM) should be quantitatively converted to product, but we and others have observed maximal substrate turnover efficiencies of 50–80%.<sup>11,25,27,28,32,44</sup> Some fraction of the labeled substrate and HJ may be incapable of reacting further, either because they are sequestered into an inaccessible complex or are chemically damaged.

In a diagnostic experiment,<sup>25,35</sup> we tested whether any products or HJs arose from the incorrect parallel arrangement of Lox during the recombination reaction. Labeled fLoxP was reacted with a 52 bp duplex containing an asymmetrically positioned LoxP site. Only HJs and products from antiparallel aligned substrates were detected. Since the reaction is under equilibrium control, it would be unlikely that parallel alignment of Lox substrates in the synaptic complex would lead to substantial production of high-energy HJ intermediate and duplex products containing base mismatches (data not shown).

#### Titration, kinetics, and suicide substrate assays

The Cre/Lox complex assembly and kinetic parameters were determined as described<sup>34</sup> and briefly outlined in Table 2. Averaged parameters ( $\pm$  standard deviation of 3–4 replicates) are reported in Table 2. Concentrations of sLox and Cre in the titration reactions were optimized for different Cre–Lox combinations as follows: fLox was  $\sim$ 1 nM in all titrations; Cre was in a 4:1 ratio with sLox substrates; for CreWT/S1rev, CreH289N/LoxP, and CreH289N/S1rev, sLox was 15, 45, 75, 90, 120, 150, 450, and 900 nM; for CreH289A/LoxP and CreH289A/S1rev, sLox was 15, 30, 60, 90, 120, 250, 600, and 1200 nM. In kinetics reactions, time points were also optimized for substrates, and varied from the CreWT/LoxP original<sup>34</sup> as follows: for CreWT/S1rev, aliquots were quenched at 15, 30, 60, 120, 240, 480, 960, and 1800 s; for CreH289N/S1rev, aliquots were quenched at 30, 60, 120, 480, 960, 1800, 3600, and 14,400 s; for CreH289A/LoxP, CreH289A/S1rev, and CreH289N/LoxP, aliquots were quenched at 60, 120, 480, 1800, 3600, 10,800, 14,400, and 23,400 s.

CreH289A/LoxP suicide substrate reactions ( $L^* + R$  and  $R^* + L$ ) were performed as described,<sup>27</sup> except that time point samples were quenched at 5, 10, 20, 40, 120, 240, 360, 480, 660, and 1500 min. Averaged kinetic constants ( $\pm$  standard deviation from three replicates) for the reactions were determined as outlined in Table 2 and by Martin *et al.*<sup>27</sup>

#### Synthetic Holliday junction resolution

For HJ resolution reactions, oligonucleotides 1–4 (purified by denaturing PAGE) correspond exactly to the sequences outlined by Lee & Sadowski, and synthetic HJs were prepared as described.<sup>30</sup> In brief, the 5' end of strand 1 was labeled with <sup>32</sup>P and purified using a Qiagen nucleotide removal kit. Strands 1–4 were annealed at 80 °C and cooled to room temperature in 100 mM NaCl and 5 mM MgCl<sub>2</sub>. The unlabeled strands (2, 3, and 4) were in fivefold excess of the labeled strand (1), at 100 nM and 20 nM, respectively.

CreWT or CreH289A (250 nM) was added to pre-formed HJ (2 nM) for 1 h at 30 °C, in 50 mM Tris–HCl

(pH 7.4), 30 mM NaCl, 2 mM MgCl<sub>2</sub>, and 3% glycerol. Reactions were quenched in 0.1% (w/v) SDS and 0.05 mg/ml Proteinase K for 30 min at 50 °C. The products were separated by non-denaturing 8% PAGE, and the gels were dried and processed as above. Reactions were performed in triplicate.

## Acknowledgements

This work was funded by a grant from the National Institutes of Health (NIGMS R01 GM63109). K.G. was supported by an NIH Training Grant (T32 GM070377). Protein purification was carried out in the W. M. Keck Protein Expression Facility at the University of California, Davis. We thank Paul Sadowski and Linda Lee for helpful discussions and early access to their review on this subject.

## Supplementary Data

Supplementary data associated with this article can be found, in the online version, at [10.1016/j.jmb.2005.08.077](https://doi.org/10.1016/j.jmb.2005.08.077)

## References

- Sherratt, D. J. & Wigley, D. B. (1998). Conserved themes but novel activities in recombinases and topoisomerases. *Cell*, **93**, 149–152.
- Wigley, D. B. (1998). Teaching a new dog old tricks? *Structure*, **6**, 543–548.
- Nunes-Duby, S. E., Kwon, H. J., Tirumalai, R. S., Ellenberger, T. & Landy, A. (1998). Similarities and differences among 105 members of the Int family of site-specific recombinases. *Nucl. Acids Res.* **26**, 391–406.
- Cheng, C., Kussie, P., Pavletich, N. & Shuman, S. (1998). Conservation of structure and mechanism between eukaryotic topoisomerase I and site-specific recombinases. *Cell*, **92**, 841–850.
- Esposito, D. & Scozza, J. J. (1997). The integrase family of tyrosine recombinases: evolution of a conserved active site domain. *Nucl. Acids Res.* **25**, 3605–3614.
- Grainge, I. & Jayaram, M. (1999). The integrase family of recombinases: organization and function of the active site. *Mol. Microbiol.* **33**, 449–456.
- Hoess, R. H. & Abremski, K. (1985). Mechanism of strand cleavage and exchange in the Cre–lox site-specific recombination system. *J. Mol. Biol.* **181**, 351–362.
- Sternberg, N. (1981). Bacteriophage P1 site-specific recombination. III. Strand exchange during recombination at lox sites. *J. Mol. Biol.* **150**, 603–608.
- Hoess, R. H., Ziese, M. & Sternberg, N. (1982). P1 site-specific recombination: nucleotide sequence of the recombining sites. *Proc. Natl Acad. Sci. USA*, **79**, 3398–3402.
- Abremski, K., Hoess, R. & Sternberg, N. (1983). Studies on the properties of P1 site-specific recombination: evidence for topologically unlinked products following recombination. *Cell*, **32**, 1301–1311.
- Abremski, K. & Hoess, R. (1984). Bacteriophage P1 site-specific recombination. Purification and properties of the Cre recombinase protein. *J. Biol. Chem.* **259**, 1509–1514.

12. Branda, C. S. & Dymecki, S. M. (2004). Talking about a revolution: the impact of site-specific recombinases on genetic analyses in mice. *Dev. Cell*, **6**, 7–28.
13. Gilbertson, L. (2003). Cre-lox recombination: Creative tools for plant biotechnology. *Trends Biotechnol.* **21**, 550–555.
14. Kolb, A. F. (2002). Genome engineering using site-specific recombinases. *Cloning Stem Cells*, **4**, 65–80.
15. Tronche, F., Casanova, E., Turiault, M., Sahly, I. & Kellendonk, C. (2002). When reverse genetics meets physiology: the use of site-specific recombinases in mice. *FEBS Letters*, **529**, 116–121.
16. Van Duyne, G. D. (2001). A structural view of cre-loxP site-specific recombination. *Annu. Rev. Biophys. Biomol. Struct.* **30**, 87–104.
17. Hoess, R., Wierzbicki, A. & Abremski, K. (1987). Isolation and characterization of intermediates in site-specific recombination. *Proc. Natl Acad. Sci. USA*, **84**, 6840–6844.
18. Hoess, R. H. & Abremski, K. (1984). Interaction of the bacteriophage P1 recombinase Cre with the recombining site loxP. *Proc. Natl Acad. Sci. USA*, **81**, 1026–1029.
19. Guo, F., Gopaul, D. N. & van Duyne, G. D. (1997). Structure of Cre recombinase complexed with DNA in a site-specific recombination synapse. *Nature*, **389**, 40–46.
20. Gopaul, D. N., Guo, F. & Van Duyne, G. D. (1998). Structure of the Holliday junction intermediate in Cre-loxP site-specific recombination. *EMBO J.* **17**, 4175–4187.
21. Guo, F., Gopaul, D. N. & Van Duyne, G. D. (1999). Asymmetric DNA bending in the Cre-loxP site-specific recombination synapse. *Proc. Natl Acad. Sci. USA*, **96**, 7143–7148.
22. Lee, L. & Sadowski, P. D. (2005). In Strand selection by the tyrosine recombinases. In *Prog. Nucleic Acid Res. Mol. Biol.* (Moldave, K., ed.), vol. 80, pp. 1–42. Academic Press, New York.
23. Hoess, R., Wierzbicki, A. & Abremski, K. (1990). Synapsis in the Cre-lox Site-specific Recombination System. In *Structure and Methods: Human Genome Initiative and DNA Recombination* (Sarma, R. & Sarma, M., ed.), vol. 1, pp. 203–213. Adenine Press, Schenectady, NY.
24. Shaikh, A. & Sadowski, P. (2000). Trans complementation of variant Cre proteins for defects in cleavage and synapsis. *J. Biol. Chem.* **275**, 30186–30195.
25. Lee, L. & Sadowski, P. D. (2003). Sequence of the loxP site determines the order of strand exchange by the Cre recombinase. *J. Mol. Biol.* **326**, 397–412.
26. Tribble, G., Ahn, Y. T., Lee, J., Dandekar, T. & Jayaram, M. (2000). DNA recognition, strand selectivity, and cleavage mode during integrase family site-specific recombination. *J. Biol. Chem.* **275**, 22255–22267.
27. Martin, S. S., Pulido, E., Chu, V. C., Lechner, T. S. & Baldwin, E. P. (2002). The order of strand exchanges in Cre-LoxP recombination and its basis suggested by the crystal structure of a Cre-LoxP Holliday junction complex. *J. Mol. Biol.* **319**, 107–127.
28. Ennifar, E., Meyer, J. E., Buchholz, F., Stewart, A. F. & Suck, D. (2003). Crystal structure of a wild-type Cre recombinase-loxP synapse reveals a novel spacer conformation suggesting an alternative mechanism for DNA cleavage activation. *Nucl. Acids Res.* **31**, 5449–5460.
29. Ghosh, K., Lau, C. K., Guo, F., Segall, A. M. & Van Duyne, G. D. (2005). Peptide trapping of the Holliday junction intermediate in Cre-loxP site-specific recombination. *J. Biol. Chem.* **280**, 8290–8299.
30. Lee, L. & Sadowski, P. D. (2001). Directional resolution of synthetic holliday structures by the Cre recombinase. *J. Biol. Chem.* **276**, 31092–31098.
31. Lee, L., Chu, L. C. & Sadowski, P. D. (2003). Cre induces an asymmetric DNA bend in its target loxP site. *J. Biol. Chem.* **278**, 23118–23129.
32. Lee, G. & Saito, I. (1998). Role of nucleotide sequences of loxP spacer region in Cre-mediated recombination. *Gene*, **216**, 55–65.
33. Hoess, R. H., Wierzbicki, A. & Abremski, K. (1986). The role of the loxP spacer region in P1 site-specific recombination. *Nucl. Acids Res.* **14**, 2287–2300.
34. Martin, S. S., Chu, V. C. & Baldwin, E. (2003). Modulation of the active complex assembly and turnover rate by protein-DNA interactions in Cre-LoxP recombination. *Biochemistry*, **42**, 6814–6826.
35. Lee, L. & Sadowski, P. D. (2003). Identification of Cre residues involved in synapsis, isomerization, and catalysis. *J. Biol. Chem.* **278**, 36905–36915.
36. Nunes-Duby, S. E., Matsumoto, L. & Landy, A. (1987). Site-specific recombination intermediates trapped with suicide substrates. *Cell*, **50**, 779–788.
37. El Hassan, M. A. & Calladine, C. R. (1997). Conformational characteristics of DNA: empirical classifications and a hypothesis for the conformational behavior of dinucleotide steps. *Phil. Trans. R. Soc. Lond. sec. A*, **335**, 43–100.
38. Packer, M. J., Dauncey, M. P. & Hunter, C. A. (2000). Sequence-dependent DNA structure: dinucleotide conformational maps. *J. Mol. Biol.* **295**, 71–83.
39. Parsons, R. L., Prasad, P. V., Harshey, R. M. & Jayaram, M. (1988). Step-arrest mutants of FLP recombinase: implications for the catalytic mechanism of DNA recombination. *Mol. Cell. Biol.* **8**, 3303–3310.
40. Jayaram, M., Crain, K. L., Parsons, R. L. & Harshey, R. M. (1988). Holliday junctions in FLP recombination: resolution by step-arrest mutants of FLP protein. *Proc. Natl Acad. Sci. USA*, **85**, 7902–7906.
41. Woods, K. C., Martin, S. S., Chu, V. C. & Baldwin, E. P. (2001). Quasi-equivalence in site-specific recombinase structure and function: crystal structure and activity of trimeric Cre recombinase bound to a three-way Lox DNA junction. *J. Mol. Biol.* **313**, 49–69.
42. Kunkel, T. A., Bebenek, K. & McClary, J. (1991). Efficient site-directed mutagenesis using uracil-containing DNA. *Methods Enzymol.* **204**, 125–139.
43. Laemmli, U. K. (1970). Cleavage of structural proteins during the assembly of the head of bacteriophage T4. *Nature*, **227**, 680–685.
44. Ringrose, L., Lounnas, V., Ehrlich, L., Buchholz, F., Wade, R. & Stewart, A. F. (1998). Comparative kinetic analysis of FLP and cre recombinases: mathematical models for DNA binding and recombination. *J. Mol. Biol.* **284**, 363–384.

Edited by J. Karn

(Received 8 June 2005; received in revised form 25 August 2005; accepted 26 August 2005)  
Available online 5 October 2005